Received: 3 April 2020 | Accepted: 31 August 2020 | Published online: 3 November 2020

DOI: 10.1002/jeq2.20160

Journal of Environmental Quality

TECHNICAL REPORTS

Surface Water Quality

Improving the effectiveness of saturated riparian buffers for removing nitrate from subsurface drainage

Andrea R. McEachran[1] | **Loulou C. Dickey**[1] | **Chris R. Rehmann**[1] | **Tyler A. Groh**[2] | **Thomas M. Isenhart**[3] | **Michael A. Perez**[4] | **Cassandra J. Rutherford**[1]

[1] Dep. of Civil, Construction, and Environmental Engineering, Iowa State Univ., Ames, IA 50011, USA

[2] Dep. of Ecosystem Science and Management, Pennsylvania State Univ., State College, PA 16801, USA

[3] Dep. of Natural Resource Ecology and Management, Iowa State Univ., Ames, IA 50011, USA

[4] Dep. of Civil and Environmental Engineering, Auburn Univ., Auburn, AL 36849, USA

Correspondence
Chris R. Rehmann, Dep. of Civil, Construction, and Environmental Eng., Iowa State Univ., Ames, IA 50011, USA.
Email: rehmann@iastate.edu

Assigned to Associate Editor Casey D. Kennedy.

Funding information
Iowa Nutrient Research Center

Abstract

A saturated riparian buffer (SRB) is an edge-of-field conservation practice that reduces nitrate export from agricultural lands by redistributing tile drainage as shallow groundwater and allowing for denitrification and plant uptake. We propose an approach to improve the design of SRBs by analyzing a tradeoff in choosing the SRB width, and we apply the approach to six sites with SRBs in central Iowa. A larger width allows for more residence time, which increases the opportunity for removing nitrate that enters the buffer. However, because the SRBs considered here treat only a portion of the tile flow when it is large, for the same difference in hydraulic head, a smaller width allows more of the total tile flow to enter the buffer and therefore treats more of the drainage. By maximizing the effectiveness of nitrate removal, defined as the ratio of total nitrate removed by the SRB to total nitrate leaving the field in tile drainage, an equation for the optimal width was derived in terms of soil properties, denitrification rates, and head difference. All six sites with existing SRBs considered here have optimal widths smaller than the current width, and two are below the minimum width listed in current design standards. In terms of uncertainty, the main challenges in computing the optimal width for a site are estimating the removal coefficient for nitrate and determining the saturated hydraulic conductivity. Nevertheless, including a width that accounts for site conditions in the design standards would improve water quality locally and regionally.

1 | INTRODUCTION

Nitrate exported from agricultural lands through artificial subsurface drainage, or tile, can impair the quality of surface waters. Tile drainage is commonly used in U.S. midwestern agriculture to improve row crop production by lowering the water table in the field to provide a well-aerated root zone. Because nitrate is easily leached, tile drainage typically has high nitrate concentrations: Baker and Johnson (1981) reported concentrations up to 61 mg N L^{-1} in tile drainage from a field in Iowa. This nitrate-rich water drains into the Mississippi River and ultimately to the northern Gulf of Mexico, contributing to the nation's largest recurring hypoxic zone. Nitrate export from agricultural tile drainage has been identified as a major contributor to this hypoxic zone (Goolsby, Battaglin, Aulenbach, & Hooper, 2001).

Because of the adverse effects of nutrient export, conservation practices have been developed to reduce nutrient flux from agricultural lands to surface waters. In-field practices (e.g., cover crops, living mulches, extended rotations,

Abbreviations: SRB, saturated riparian buffer; WSS, Web Soil Survey.

fertilizer management, and nitrification inhibitors) reduce nitrate loss; however, they can be difficult and costly to implement, and alone they cannot meet the targets of nutrient reduction strategies (IDALS, IDNR, & ISU, 2017). Therefore, edge-of-field practices (e.g., bioreactors, constructed wetlands, and riparian buffers) are also used to reduce nitrate flux to surface waters. Riparian buffers effectively remove sediment and nutrients from surface runoff and nitrate from shallow subsurface flow (Groh, Isenhart, & Schultz, 2020). However, because riparian buffers and tile drainage are not hydraulically connected, nitrate-rich tile drainage bypasses treatment in the riparian buffer. Thus, traditional riparian buffers are less effective for removing nitrate in regions with tile drainage, which accounts for up to 50% of cropland in U.S. midwestern states (Kalita, Cooke, Anderson, Hirschi, & Mitchell, 2007).

Tile drainage can be treated with saturated riparian buffers (SRBs), an edge-of-field conservation practice introduced in 2010 (Jaynes & Isenhart, 2014). Saturated riparian buffers intercept tile drainage at a control structure that redirects a portion of the flow into a perforated distribution pipe that runs parallel to the receiving stream and distributes flow as shallow groundwater through a vegetated riparian buffer. In this way, SRBs facilitate nitrate removal through microbial denitrification, plant uptake, and microbial immobilization (Jaynes & Isenhart, 2014). Of these three processes, denitrification is the primary removal mechanism in SRBs (Groh, Davis, Isenhart, Jaynes, & Parkin, 2019a), and, because denitrification depends on the available organic carbon (Hill & Cardaci, 2004), SRBs take advantage of the high organic carbon concentrations in the upper horizons of the soil profile (Jaynes & Isenhart, 2014) by raising the water table using the control structure.

Because SRBs are relatively new, questions remain regarding the most effective design. The removal effectiveness, or the ratio of nitrate removed by the SRB to the total nitrate leaving the field in the tile, can be quite high; values from six sites monitored in Iowa ranged from 7 to 92% (Jaynes & Isenhart, 2019a). The effectiveness depends on the flow from the field and site conditions such as SRB dimensions, soil characteristics, site geology, and stream conditions. Saturated riparian buffer design seeks to maintain an adequate residence time to allow for nitrate removal. However, during periods of high flow, the flow that the SRB can handle—which is controlled by the width L_x of the SRB, saturated hydraulic conductivity K, and the difference between the water level h_1 at the distribution pipe and the water level h_2 at the stream (Figure 1)—might not be large enough. In that case, some of the untreated tile drainage bypasses the SRB and flows directly to the stream. For example, Jaynes and Isenhart (2019a) found that, on average, 6–79% of the tile drainage exceeded the capacity of the six SRBs studied and flowed to the stream untreated.

Core Ideas

- A wider saturated riparian buffer does not necessarily mean more nitrate will be removed.
- The optimal width maximizes flow while maintaining adequate residence time.
- The optimal width can be smaller than the width listed in current design standards.

Therefore, a tradeoff exists in choosing the SRB width L_x. Because residence time increases with increasing width, a larger width allows more time for nitrate removal. However, assuming the initial hydraulic head set by the control structure remains constant, a larger width reduces the hydraulic gradient and consequently the total flow received by the SRB. The modeling of Jaynes and Isenhart (2019b) supports this intuition: lateral infiltration rates were higher when the distribution pipe was located closer to the stream. The USDA-NRCS Saturated Buffer Conservation Practice Standard (Code 604) guides the design of SRBs and specifies a minimum buffer width of 9.1 m (USDA-NRCS, 2016). It also specifies the minimum design flow as "five percent of drainage system capacity or as much as practical based on the available length of the vegetated buffer." However, low nitrate concentrations in monitoring wells nearest to the stream (Jaynes & Isenhart, 2014) suggest that a narrower SRB could accommodate greater flow while still removing most of the diverted nitrate.

In this study, this tradeoff was analyzed using a mass balance to determine the optimal width for SRB design by maximizing the effectiveness of nitrate removal. The width at

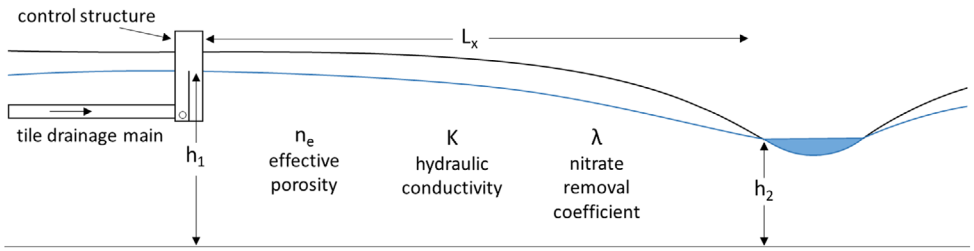

FIGURE 1 Profile view of a saturated riparian buffer with parameters defined. The overflow pipe is not shown

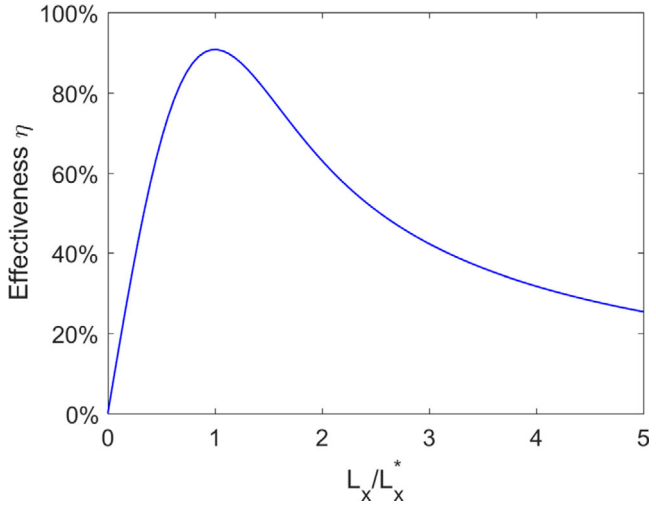

FIGURE 2 Effectiveness is maximized when the saturated riparian buffer width L_x is equal to the optimal width L_x* (i.e., when L_x/L_x* = 1)

six existing sites was compared with the theoretical optimal width to determine how standard SRB design guidance could be modified to increase the effectiveness and to what extent the effectiveness can be improved. Challenges in estimating the parameters needed to compute the optimal width are discussed, and approaches for estimating these parameters are assessed.

2 | MATERIALS AND METHODS

2.1 | Theoretical calculations

The optimal SRB width is determined by maximizing the nitrate removal effectiveness of the SRB (Figure 2), defined as the ratio of total nitrate removed by the SRB to total nitrate leaving the field in the tile drainage. If $\dot{m}_{in}$ and $\dot{m}_{out}$ are the mass fluxes of nitrate entering the control structure and leaving the SRB, respectively, then the removal effectiveness η is

$$\eta = 1 - \frac{\dot{m}_{out}}{\dot{m}_{in}} \tag{1}$$

The mass flux of nitrate into the SRB consists of all of the nitrate in the tile drainage that enters the control structure. The mass flux of nitrate leaving the SRB includes nitrate that bypasses the SRB and nitrate that is not removed in the SRB. Therefore, the effectiveness can be expressed in terms of flow rates and concentrations:

$$\eta = \frac{Q}{Q_t}\left(1 - \frac{C_{out}}{C_t}\right) \tag{2}$$

where Q is the flow entering the SRB, Q_t is the flow from the tile drainage in the field, C_{out} is the nitrate concentration in groundwater leaving the SRB, and C_t is the initial nitrate concentration of the tile drainage. We emphasize that, because some flow can bypass the buffer and flow to the stream, $Q/Q_t \leq 1$. For steady one-dimensional flow through homogeneous soil, Darcy's law gives

$$Q = K\frac{h_1^2 - h_2^2}{2L_x}L_y \tag{3}$$

where L_y is the length of the distribution pipe. Darcy's law applies because conservative estimates of the particle size (0.5 mm), travel time (20 d), effective porosity (0.3), and SRB width (24 m) yield a Reynolds number of 2×10^{-3}, much less than the limit of 1 for validity (Fetter, 2000). With removal modeled as first-order with a removal coefficient λ, the concentration C_{out} is:

$$C_{out} = C_t \exp\left(-\lambda T_u\right) \tag{4}$$

where T_u is the time for water to travel a distance L_x in an unconfined aquifer:

$$T_u = \frac{4}{3}\frac{n_e L_x^2}{K}\frac{h_1^3 - h_2^3}{\left(h_1^2 - h_2^2\right)^2} \tag{5}$$

and n_e is the effective porosity. Equations 3–5 illustrate the tradeoff discussed in the Introduction: a smaller width L_x increases the flow through the SRB, but a larger width increases the travel time and therefore decreases the concentration in cases that are not already nitrate limited. In other words, when the width is smaller than optimal (i.e., left of the peak in Figure 2), the SRB cannot remove enough nitrate. When it is larger than optimal (i.e., right of the peak in Figure 2), it removes all of the nitrate before the end is reached, and it could accommodate a larger fraction of the tile flow.

The optimal width L_x^* is calculated by differentiating the effectiveness with respect to L_x and solving for the value of L_x that makes the derivative zero:

$$L_x^* = 0.97\left(\frac{K}{n_e\lambda}\frac{\left(h_1^2 - h_2^2\right)^2}{h_1^3 - h_2^3}\right)^{\frac{1}{2}} \tag{6}$$

The value of the effectiveness at the optimal width η* is

$$\eta^* = 0.37\frac{L_y}{Q_t}\left[\lambda n_e K\left(h_1^3 - h_2^3\right)\right]^{\frac{1}{2}} \tag{7}$$

When the difference in hydraulic head $\Delta h = h_1 - h_2$ is small, the SRB can be treated as a confined aquifer, and the optimal

TABLE 1 Characteristics of the six study sites

Characteristics	Site					
	BC-1	IA-1	B-T	HG	BC-2	SH
Installation date	Oct. 2010	June 2013	Sept. 2014	Oct. 2015	Oct. 2015	May 2016
Drainage area, ha	10.1/5.9[a]	4.7	7.1	21.8	40.5	3.4
Saturated riparian buffer width, m	21	24	11	14	22	19
Distribution pipe length, m	335	308	115	125	168	266
Number of monitoring wells	18	16	9	6	9	6
Number of slug tests	24	4	3	1	14	12
Average annual flow and nitrate removal parameters						
Precipitation, mm yr^{-1}[b]	880	937	911	866	927	965
Days with tile flow[b]	143	145	101	206	280	197
Total tile flow, mm yr^{-1}[b]	290	191	51	170	464	451
Tile flow diverted to the SRB,[b] %	42	94	51	23	21	49
Total NO_3 load removed,[b] %	39	84	48	25	8	17
Diverted NO_3 load removed,[b] %	97	91	92	99	35	36
Denitrification rate, mg N m^{-3} d^{-1}[c]	0.00–2,465	0.04–243.9	NA[d]	NA	0.08–141.8	1.44–110.2

[a]Drainage area was reduced in fall 2013. [b]From year of installation through 2017 (Jaynes & Isenhart, 2019a). [c]Range of denitrification rates from the subsurface (20–100 cm) (data from Groh et al., 2019a except SH [T. A. Groh, personal communication, 2019]). [d]NA, not available.

width in Equation 6 can be simplified to

$$L_x^* = 1.12\left(\frac{K\Delta h}{n_e\lambda}\right)^{\frac{1}{2}} \quad (8)$$

The approximation leading to Equation 8 is accurate to 3% when $\Delta h/h_2 < 0.85$. All variables are listed in Supplemental Table S1.

2.2 | Study sites

Six existing SRBs (BC-1, IA-1, B-T, HG, BC-2, and SH), all located in central Iowa, were investigated to compare their current width with their optimal width. All six SRBs receive tile drainage from fields in a corn (*Zea mays* L.) and soybean [*Glycine max* (L.) Merr.] rotation, and they are similar in their intended function and the monitoring equipment at the site. However, the SRBs vary in width, distribution pipe length, drainage area, topography, flow rates, and nitrate removal parameters (Table 1). The variety of parameters and conditions in the study sites means that the optimal width will also vary by site.

2.3 | Determining values of parameters

Computing the optimal width and effectiveness in general requires estimates of the tile flow from the field, K, effective porosity, hydraulic heads, and removal coefficient. Because our analysis involves the ratio of the effectiveness at the original width and the effectiveness at the optimal width, the tile flow is not needed. Saturated hydraulic conductivity was determined through slug tests using the Hvorslev method (Hvorslev, 1951). Slug tests measure the local K by displacing water in a well and monitoring the change in water level over time. The Hvorslev method involves fitting the water level displacement versus time data to determine t_{37}, which is the time required for the water level to equal 37% of the change from the static water level. Saturated hydraulic conductivity is then computed as

$$K = \frac{r^2 \ln\left(\frac{L}{R}\right)}{2Lt_{37}} \quad (9)$$

where r is the radius of the well, and L and R are the length and radius of the well screen, respectively. The effective porosity n_e was assumed to be equal to values used in previous studies in the watershed containing sites BC-1 and BC-2 (Fowle, 2003; D.B. Jaynes, personal communication, 2019).

Estimating the hydraulic head is challenging because the depth of the confining layer is difficult to determine. However, if Equation 8 applies, then only the difference in hydraulic head is needed. To assess the validity of Equation 8, $\Delta h/h_2$ was calculated for BC-1 because it has the most available data. The difference in head between the distribution pipe and the stream was calculated using the design head depth and depth to the stream surface in Table 1 of Jaynes and Isenhart (2019a). The depth to the confining layer—and thus h_2, the hydraulic head at the stream—was estimated by

analyzing electrical resistivity, which correlates to soil types (Wineland, 2002). The value of $\Delta h/h_2$ for BC-1 is approximately 0.3; therefore, applying Equation 8 will result in less than a 3% error. The other five sites are assumed to also have $\Delta h/h_2 < 0.85$, and the aquifers are treated as confined.

The removal coefficient λ was determined from measurements of nitrate concentrations in the monitoring wells at each site using

$$C = C_t \exp\left(-\frac{\lambda x}{v_l}\right) \tag{10}$$

where C is the nitrate concentration at distance from the distribution pipe x, and v_l is the average linear velocity of groundwater, which is calculated as

$$v_l = \frac{K\Delta h}{n_e L_x} \tag{11}$$

The removal coefficient was calculated for each date in which nitrate samples were collected. Mean values of λ are highest in fall and lowest in either spring or winter; to obtain a representative removal coefficient, the values of λ for all available sampling dates were averaged. Only values from fits with $R^2 > .3$ were used; the amount of data used ranged from 67 to 100% at each of the sites.

Although nitrate data were available in this study because the SRBs were already installed, these data will not likely be available during the SRB design phase. Therefore, because denitrification is the primary mechanism of nitrate removal in SRBs (Groh et al., 2019a), a denitrification model can be used to estimate the removal coefficient λ. Reviewing more than 50 models, Heinen (2006a) provided two versions of the actual denitrification rate D_a: for saturated conditions in which $6 < \text{pH} < 8$, the actual denitrification rate is

$$D_a = D_p \frac{C}{K_s + C} f_T \tag{12a}$$

if the reaction follows Michaelis–Menten kinetics and

$$D_a = k_d C f_T \tag{12b}$$

if the reaction is first order. In Equations 12a and 12b, D_p is the potential denitrification rate (i.e., at optimal conditions), K_s is the half-saturation constant, and f_T is a function accounting for effects of temperature. When the nitrate concentration is large ($C \gg K_s$), Equation 12a predicts that the denitrification rate is constant, or zeroth-order, but when $C \ll K_s$, Equations 12a and 12b are similar, so that the removal coefficient can be written as

$$\lambda = k_d f_T = \frac{D_p}{K_s} f_T \tag{13}$$

where k_d is a first-order denitrification coefficient. Heinen (2006a) specified the temperature function as $f_T = Q_{10}^{(T-T_r)/10}$, where T is the soil temperature (°C), T_r is a reference temperature (°C), and Q_{10} is a factor with typical values of between 2 and 3. We use Equation 13 in computing the optimal width and discuss its applicability in the next section. We take $Q_{10} = 2.5$ and $T_r = 20$ °C. Table 3 of Heinen (2006a) presents values of k_d used in six different models, ranging from 0.001 to 1.08 d^{-1}.

Because the input parameters are uncertain, the uncertainty of optimal width was computed by propagating the uncertainty in parameters in Equation 8 with a first-order analysis:

$$\left(\Delta L_x^*\right)^2 = \sum_{i-1}^{n} \left(\frac{\partial L_x^*}{\partial y_i}\Delta y_i\right)^2 = \sum_{i-1}^{n} \left(S_{y_i}\frac{\Delta y_i}{y_i}\right)^2 \tag{14}$$

where y_i indicates the dependent parameter, Δy_i is the uncertainty in y_i, and $S_y = (y_i/L_x^*)(\partial L_x^*/\partial y_i)$ is the sensitivity of the optimal width to parameter y_i. Because the magnitude of the relative sensitivity is 1/2 for all four parameters used to compute the optimal width in Equation 8, differences in contributions to the overall uncertainty in the optimal width depend only on the uncertainty in the parameters. To account for error from measurements and assumptions in the model, relative uncertainties of 100, 50, 20, and 10% were introduced for λ, K, n_e, and Δh, respectively.

3 | RESULTS AND DISCUSSION

The optimal width and its dependence on the parameters have a physical explanation that agrees with intuition. As noted in the Introduction, the optimal width arises from a balance between making the SRB wide enough that nitrate is removed and making it narrower to increase the hydraulic gradient and the flow diverted to the SRB. Therefore, the width should yield a travel time that is comparable to the removal time, or $T_u \sim \lambda^{-1}$. This balance reproduces the optimal width in Equation 8, up to a multiplicative coefficient, and the full calculation shows that the coefficient is order one. The dependence of the optimal width on the parameters also makes physical sense. A wider SRB is needed when the removal time is larger (i.e., λ is small) than the travel time. Water will flow most quickly through buffers with more conductive and less porous soils with larger head differences. The analysis provides physical basis for setting the minimum SRB width.

For all six sites, the optimal width is smaller than the current width of the SRB (Figure 3). The widths at four of the six sites exceed the upper limits of the optimal width ranges. For example, the SRB at BC-1, which is 21 m wide, is at least 4 m too wide to remove nitrate optimally. As noted in the discussion of Figure 2, at these sites nitrate concentrations

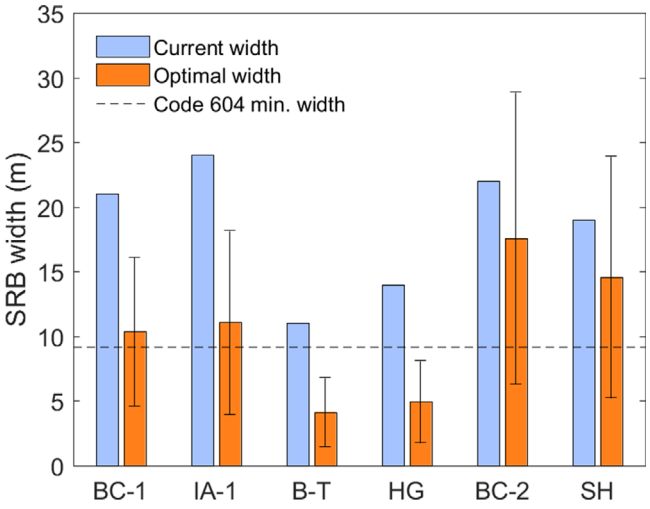

FIGURE 3 Current versus optimal saturated riparian buffer (SRB) width for the six study sites. Error bars on the optimal width result from the uncertainty analysis; each SRB has a 57% uncertainty in the optimal width. The minimum buffer width specified by current Code 604 is 9.1 m (USDA-NRCS, 2016)

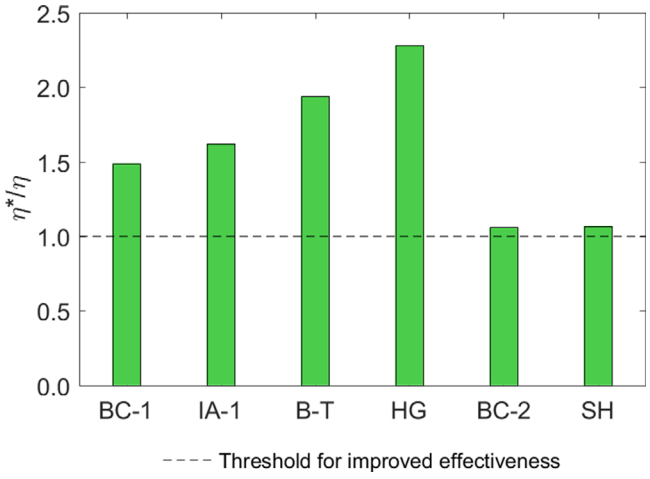

FIGURE 4 Ratio of effectiveness at the optimal width η* versus effectiveness at the current width η. A value >1 indicates a greater effectiveness at the optimal width

fall to zero before the end of the buffer is reached and the buffers could accommodate more of the tile flow. As a result, the effectiveness of nitrate removal could be about 50–120% greater at these four sites (Figure 4). The widths of the SRBs at the other two sites (BC-2 and SH) fall within the optimal width range (Figure 3), and the effectiveness is close to optimal (Figure 4). Two of the study sites (B-T and HG) have optimal widths below the current minimum buffer width listed in USDA-NRCS Code 604 (Figure 3). Because the upper limit for the optimal width of these sites is also below the 9.1 m minimum, these sites could not have been designed for maximum nitrate removal under existing design guidance. In these cases, current standards and the common practice of making SRBs wide reduce SRB effectiveness.

The trends in the optimal width and effectiveness align well with the results from a study of the denitrification potential at three of the sites. When Groh, Davis, Isenhart, Jaynes, and Parkin (2019b) added carbon as dextrose to soil cores from BC-1, BC-2, and IA-1, denitrification potential rates increased significantly for BC-2 but not for IA-1 or BC-1 cores taken further from the distribution pipe. They concluded that carbon limited denitrification at BC-2, whereas nitrate limited denitrification at BC-1 and IA-1. Calculations of the optimal width and effectiveness support these conclusions: BC-2 is operating at near-optimal effectiveness, whereas BC-1 and IA-1 could remove more nitrate (Figure 4). The nitrate-limited sites may benefit from having a distribution pipe closer to the stream (Figure 3).

The overall uncertainty of the optimal width is quite large because of uncertainty in the parameters used to calculate the optimal width. In relative terms, the optimal width is equally sensitive to all parameters in the approximate expression, Equation 8. Combining the uncertainty of all parameters yields an overall 57% uncertainty in L_x^*. The removal coefficient λ contributes 77% of the uncertainty in L_x^*. Therefore, the most effective way to reduce uncertainty in L_x^* is to improve methods of determining the removal coefficient. The second-largest source of uncertainty in L_x^* is K, with a 19% contribution to the total uncertainty, whereas n_e and Δh contribute only 3 and 0.8%, respectively. These percent uncertainties apply to each site. Although the resulting uncertainty is large, Equation 8 still provides guidance for designing effective SRBs.

Determining the removal coefficient is difficult because of the substantial uncertainty in the parameters for the denitrification model. For the sites considered in this study, the removal coefficient could be determined with greater certainty using nitrate samples from the monitoring wells. For a new site, this type of data will not likely be available, and a denitrification model such as Equation 13 must be used. Methods of measuring potential denitrification rates D_p are quite difficult and time consuming, and the wide range of values they yield, especially in areas with heterogeneity, make specifying a single representative value challenging. For example, the denitrification rates for the 20-to-100-cm depth at BC-1, BC-2, and IA-1 were in the ranges of 0.00–2,465, 0.08–141.8, and 0.04–243.9 mg N m^{-3} d^{-1}, respectively (Table 1). A denitrification model applied to eight different data sets with sand, loam, and peat soils gave potential denitrification rates ranging from 2,679 to 38,500 g N ha^{-1} d^{-1} and values of half-saturation coefficient K_s ranging from 0.46 to 135.3 mg N kg^{-1}; ranges for the two parameters were large even within the same soil types (Heinen, 2006b). The removal coefficient λ can also be estimated using Equation 13 and Table 3 of Heinen (2006a), which gives k_d in the range 0.001–1.08 d^{-1}

TABLE 2 Optimal width parameters

Site	*K* from slug tests	*K* from Web Soil Survey	n_e	Δh	λ	k_d
	m d^{-1}			m	d^{-1}	
BC-1	0.52	0.49	0.1	1.38	8.34×10^{-2}	2.75×10^{-1}
IA-1	1.35	0.33	0.1	1.80	2.49×10^{-1}	8.18×10^{-1}
B-T	4.76	0.26	0.1	1.34	4.66×10^{0}	1.53×10^{1}
HG	1.53	0.75	0.1	2.83	2.22×10^{0}	7.30×10^{0}
BC-2	0.40	0.78	0.1	1.59	2.59×10^{-2}	8.53×10^{-2}
SH	0.43	0.42	0.1	1.59	4.01×10^{-2}	1.32×10^{-1}

Note. *K*, saturated hydraulic conductivity; Δh, difference in hydraulic head; k_d, first-order denitrification coefficient computed from the nitrate removal coefficient λ using $Q_{10} = 2.5$, $T = 7$ °C, and $T_r = 20$ °C; n_e, effective porosity.

and lists several sources for $k_d \approx 0.1$ d^{-1}. For four of our study sites, k_d computed from Equation 13 was within the range of 0.085–0.818 d^{-1} (Table 2), which lies in the range from Heinen (2006a). The other two sites yield a much larger k_d (7.3 and 15.3 d^{-1}) because the removal coefficient was one to two orders of magnitude larger at these sites.

Two assumptions add to the uncertainty in the removal coefficient. The calculations of λ assume that nitrate removal occurs by a first-order reaction. As noted in the discussion of Equations 12a and 12b, first-order kinetics requires nitrate concentrations much smaller than the half-saturation coefficient K_s; in particular, the error in the actual denitrification rate is about 17% when $C/K_s = 0.5$ and 50% when $C/K_s = 1$, and accounting for the plateau in the denitrification rate at high concentrations would yield a larger required buffer width. In a study of denitrification beds (Ghane, Fausey, & Brown, 2015) and in a study of wetlands (Messer, Burchell, & Bírgand, 2017), a first-order model better fit nitrate removal than a zeroth-order model did. Many values of K_s in soil have been reported, including 0.5 mg L^{-1} (Kinzelbach & Schäfer, 1991), 0.89 mg L^{-1} (Killingstad, Widdowson, & Smith, 2002), and 10 mg L^{-1}, which is used in three of the models reviewed by Heinen (2006a). The value $K_s = 10$ mg L^{-1} is comparable to or lower than many concentrations measured in the field tile and closest well in the dataset presented by Jaynes and Isenhart (2014), but most concentrations farther from the control structure are much lower and often below the 0.3 mg L^{-1} detection limit. Therefore, although the removal is better modeled with Michaelis–Menten kinetics near the control structure, a first-order model works well in most of the SRB.

Another assumption that affects uncertainty in the removal coefficient involves unsteadiness in the fate and transport of nitrate. Equation 10, which was used to compute λ, holds for steady state. Because it was applied to concentration profiles measured on several days, the analysis essentially assumes a quasi-steady state in which flow and contaminant processes were constant over the time required to establish the concentration profile. For these sites, that time is about 10–20 d. Continuous records at BC-1, for example, show periods in which the flow and water levels are approximately constant for times on this order (Jaynes & Isenhart, 2014); however, many high-runoff events with rapidly varying flow and water levels also occur. Accounting for these variations in more detail would involve deriving an unsteady form of Equation 10 by solving a one-dimensional diffusion equation for the head (e.g., de Marsily, 1986, section 8.5), computing the average linear velocity, and solving the transport equation for nitrate, likely with a numerical method.

The saturated hydraulic conductivity plays a significant role in determining the optimal width, yet it can be challenging to determine, especially in regions with heterogeneity. In the design of a new SRB, the saturated hydraulic conductivity could be estimated from the Web Soil Survey (WSS) of the USDA-NRCS. Saturated hydraulic conductivities from slug tests matched those from WSS well at BC-1 and SH, they were within a factor of about 2 at BC-2 and HG, and they differed by more at IA-1 and B-T (Table 2). The differences at IA-1 and B-T could be due to the straightening of the channel at these two sites and the smaller number of slug tests available ($n = 3$ at B-T, $n = 4$ at IA-1; Table 1). Although the analysis leading to Equations 6 and 8 treats the aquifer as homogeneous, alluvial soils tend to be layered, and meanders can lead to horizontal heterogeneity. To some extent, the slug tests provide an effective conductivity that accounts for vertical variations in soil properties, but, because they typically measure within a few meters of the well (Fetter, 2000), they can miss horizontal variations. The good agreement between the slug tests and WSS at sites BC-1 and SH, at which every well was sampled at least twice (Table 1), suggests that if soil testing is done at a candidate site, it should be done at several locations in the buffer.

In deriving the equation for the optimal width, dispersion was neglected. Hydrodynamic dispersion in groundwater is quantified by the longitudinal dispersivity a_L, and, because it depends on the scale of the flow (Schulze-Makuch, 2005; Xu & Eckstein, 1995), a calculation of the optimal width of the SRB that includes dispersion would be iterative. The error

in determining the removal coefficient λ with Equation 10 is proportional to the parameter $a_L\lambda/v_1$; applying the formula of Schulze-Makuch (2005) to the six SRB sites suggests an error of 8–75% in λ. However, because the scatter in dispersivities is large (Schulze-Makuch, 2005) and the resulting underprediction of the optimal width, which depends on $\lambda^{1/2}$ (Equation 8), is 4–32%, dispersion is omitted from the analysis for simplicity.

Allowing SRBs to be narrower than the width of 9.1 m specified in Code 604 would result in removing more of the nitrate load because it would reduce the constraints for designing SRBs to remove nitrate most optimally. A smaller width is beneficial at sites with less conductive soils, little topographic relief, large effective porosities, and/or large removal rates. Although the length of the distribution pipe and the tile flow rate do not affect the optimal width, they do control the SRB's effectiveness. A longer distribution pipe and a lower tile flow rate increase SRB effectiveness. In other words, for high flow spread through a short distribution pipe, the SRB can be operating optimally, but the flow might be large enough that the effectiveness is low due to nitrate bypassing the SRB. Although obtaining the parameters required to compute the optimal width is challenging, using Equation 8 to approximate the optimal width would be useful in determining an effective design.

Designing SRBs to be narrower may cause concerns related to treating runoff, providing habitat for wildlife, and maintaining the slope stability of the streambank. Because the width of a riparian buffer can differ from the width of the SRB, both practices can be optimally designed at the same site: the distribution pipe does not need to be located at the edge of the riparian buffer. Therefore, surface runoff treatment and wildlife habitat can be preserved as functions of a site for a saturated riparian buffer. Increased flow and an elevated water table can reduce the stability of a slope, but an assessment of slope stability for five SRB sites (BC-1, IA-1, B-T, BC-2, and SH) showed that four of the slopes would be stable at widths greater than 3 m (Dickey et al., 2020), a distance smaller than all of the optimal widths in Figure 3. The fifth site (BC-2) has a factor of safety below the acceptable threshold for slope stability even without added flow. We recommend not placing SRBs on slopes already prone to failure.

4 | CONCLUSIONS

We have described an approach for choosing the width of a saturated riparian buffer more systematically than under current standards. Intuition suggests using a larger width to remove nitrate most effectively because a larger width will allow more time for denitrification, plant uptake, and microbial immobilization to take place and will increase the likelihood of hitting hot spots and hot moments of denitrification. We have shown that although a larger width will decrease the nitrate concentration of the drainage that leaves the SRB as groundwater, it will also increase the nitrate load that will overflow to the stream without treatment. Balancing the time to remove nitrate and the time for water to flow through the SRB leads to a quantitative expression for the optimal width. A key remaining challenge is to develop better ways to predict nitrate removal so that more effective SRBs can be designed and implemented.

ACKNOWLEDGMENTS

The authors thank Kent Heikens for help with field measurements and Dan Jaynes for providing data and insight on saturated riparian buffers. This work was supported by a grant from the Iowa Nutrient Research Center.

CONFLICT OF INTEREST

The authors declare no conflict of interest.

ORCID

Andrea R. McEachran https://orcid.org/0000-0002-9153-3894

Chris R. Rehmann https://orcid.org/0000-0002-4740-557X

REFERENCES

Baker, J. L., & Johnson, H. P. (1981). Nitrate-nitrogen in tile drainage as affected by fertilization. *Journal of Environmental Quality*, *10*(4), 519–522. https://doi.org/10.2134/jeq1981.00472425001000040020x

de Marsily, G. (1986). *Quantitative hydrogeology*. San Diego, CA: Academic Press.

Dickey, L. C., McEachran, A. R., Rutherford, C. J., Perez, M. A., Rehmann, C. R., Groh, T. A., … Jaynes, D. B. (2020). Slope stability analysis of saturated riparian buffers. In *Proceedings of the 20th Annual International Erosion Control Association Environmental Connection 20 Conference*, Raleigh, NC. Retrieved from https://www.eventscribe.com/2020/IECA/fsPopup.asp?efp=RktZTlpURlk1NjEz&PresentationID=602788&rnd=0.2624815&mode=presinfo

Fetter, C. W. (2000). *Applied hydrogeology* (4th ed.). London: Pearson.

Fowle, C. J. (2003). *Application of an analytic element model to understanding groundwater flow and nitrate flux in the Bear Creek watershed in central Iowa* (Master's thesis). Iowa State University. Retrieved from https://lib.dr.iastate.edu/cgi/viewcontent.cgi?article=20964&context=rtd

Ghane, E., Fausey, N. R., & Brown, L. C. (2015). Modeling nitrate removal in a denitrification bed. *Water Research*, *71*, 294–305. https://doi.org/10.1016/j.watres.2014.10.039

Goolsby, D. A., Battaglin, W. A., Aulenbach, B. T., & Hooper, R. P. (2001). Nitrogen input to the Gulf of Mexico. *Journal of Environmental Quality*, *30*(2), 329–336. https://doi.org/10.2134/jeq2001.302329x

Groh, T. A., Davis, M. P., Isenhart, T. M., Jaynes, D. B., & Parkin, T. B. (2019a). In situ denitrification in saturated riparian buffers. *Journal of Environmental Quality*, *48*(2), 376. https://doi.org/10.2134/jeq2018.03.0125

Groh, T. A., Davis, M. P., Isenhart, T. M., Jaynes, D. B., & Parkin, T. B. (2019b). Denitrification potential in three saturated riparian buffers. *Agriculture Ecosystems and Environment*, *286*, 106656. https://doi.org/10.1016/j.agee.2019.106656

Groh, T. A., Isenhart, T. M., & Schultz, R. C. (2020). Long-term nitrate removal in three riparian buffers: 21 years of data from the Bear Creek watershed in central Iowa. *Science of the Total Environment*, *740*, 140114. https://doi.org/10.1016/j.scitotenv.2020.140114

Heinen, M. (2006a). Simplified denitrification models: Overview and properties. *Geoderma*, *133*(3–4), 444–463. https://doi.org/10.1016/j.geoderma.2005.06.010

Heinen, M. (2006b). Application of a widely used denitrification model to Dutch data sets. *Geoderma*, *133*, 464–473. https://doi.org/10.1016/j.geoderma.2005.08.011

Hill, A. R., & Cardaci, M. (2004). Denitrification and organic carbon availability in riparian wetland soils and subsurface sediments. *Soil Science Society of America Journal*, *68*(1), 320–325. https://doi.org/10.2136/sssaj2004.0320

Hvorslev, M. J. (1951). *Time lag and soil permeability of groundwater observations* (Bulletin 36). Vicksburg, MS: U.S. Army Corps of Engineers Waterways Experimental Station.

IDALS, IDNR, & ISU. (2017). *Iowa nutrient reduction strategy*. Iowa State University. Retrieved from www.nutrientstrategy.iastate.edu/documents

Jaynes, D. B., & Isenhart, T. M. (2014). Reconnecting tile drainage to riparian buffer hydrology for enhanced nitrate removal. *Journal of Environmental Quality*, *43*(2), 631–638. https://doi.org/10.2134/jeq2013.08.0331

Jaynes, D. B., & Isenhart, T. M. (2019a). Performance of saturated riparian buffers in Iowa, USA. *Journal of Environmental Quality*, *48*(2), 289–296. https://doi.org/10.2134/jeq2018.03.0115

Jaynes, D. B., & Isenhart, T. M. (2019b). Increasing infiltration into saturated riparian buffers by adding additional distribution pipes. *Journal of Soil and Water Conservation*, *74*(6), 545–553. https://doi.org/10.2489/jswc.74.6.545

Kalita, P. K., Cooke, R. A. C., Anderson, S. M., Hirschi, M. C., & Mitchell, J. K. (2007). Subsurface drainage and water quality: The Illinois experience. *American Society of Agricultural and Biological Engineers*, *50*(5), 1651–1656.

Killingstad, M. W., Widdowson, M. A., & Smith, R. L. (2002). Modeling enhanced in situ denitrification in groundwater. *Journal of Environmental Engineering*, *128*(6), 491–504. https://doi.org/10.1061/(asce)0733-9372(2002)128:6(491)

Kinzelbach, W., & Schäfer, W. (1991). Numerical modeling of natural and enhanced denitrification processes in aquifers. *Water Resources Research*, *27*(6), 1123–1135. https://doi.org/10.1029/91WR00474

Messer, T. L., Burchell, M. R., & Bírgand, F. (2017). Comparison of four nitrate removal kinetic models in two distinct wetland restoration mesocosm systems. *Water*, *9*(9), 635. https://doi.org/10.3390/w9070517

Schulze-Makuch, D. (2005). Longitudinal dispersivity data and implications for scaling behavior. *Ground Water*, *43*(3), 443–456. https://doi.org/10.1111/j.1745-6584.2005.0051.x

USDA-NRCS. (2016). *Conservation practice standard for saturated buffers: Code 604*. Washington, DC: USDA-NRCS.

Wineland, T. R. (2002). *Assessing the role of geology for nitrate fate and transport in groundwater beneath riparian buffers* (Master's thesis). Iowa State University.

Xu, M., & Eckstein, Y. (1995). Use of weighted least-squares method in evaluation of the relationship between dispersivity and field scale. *Groundwater*, *33*(6), 905–908. https://doi.org/10.1111/j.1745-6584.1995.tb00035.x

SUPPORTING INFORMATION

Additional supporting information may be found online in the Supporting Information section at the end of the article.

How to cite this article: McEachran AR, Dickey LC, Rehmann CR, et al. Improving the effectiveness of saturated riparian buffers for removing nitrate from subsurface drainage. *J. Environ. Qual.* 2020;49:1624–1632. https://doi.org/10.1002/jeq2.20160